Isopolyniobotungstate $H_xNb_2W_4O_{19}^{(4-x)-}$ Ions: Analysis of the State of the Ions in Aqueous Solutions, Formation Constants Calculation and Thallium Salts Synthesis

Svetlana M. Vavilova,[1] Maksym A. Kryuchkov,[2] Katerina E. Belousova[1] and Georgiy M. Rozantsev[1]

[1] *Department of Inorganic chemistry, Faculty of Chemistry, Donetsk National University, 24 Universitetskaya Str., Donetsk 83001, Ukraine*

[2] *Department of Chemistry, University of Montreal, Montreal H3T 2BI, Canada*

* *Corresponding author: E-mail: razantsev @dongu.donetsk.ua*

Abstract

By means of pH-potentiometric titration, the processes of the complexes formation in the system $Nb_6O_{19}^{8-}-WO_4^{2-}-H^+-H_2O$ with $C_{Nb} : C_W = 2 : 4$ was studied at different Nb + W concentrations. Exerimental data, being processed by mathematical modeling, allowed to obtain the distribution diagrams of individual niobium and tungsten isopoly anions, and mixed isopolyniobotungstates in the range of $Z = C_H^0/C_{Nb+W}^0 = 0 – 2.0$ (background electrolyte is NaCl). Concentrational and thermodynamic formation constants were calculated using quasi–*Neuton* method (CLINP 2.1 software) and it was shown, that the formation of isopolyniobotungstates ($H_xNb_2W_4O_{19}^{(4-x)-}$, $x = 0 – 2$) of the 6th row of Periodic table proceeds through intermediate $Nb_3W_3O_{19}^{5-}$ ion formation. Thallium salts $Tl_3HNb_2W_4O_{19} \cdot 10H_2O$ and $Tl_2H_2Nb_2W_4O_{19} \cdot 10H_2O$ were isolated and characterized by elemental and EDX spectral analysis, electron microscopy and FTIR-spectroscopy.

Keywords: Polyoxometalates, isopolyniobotungstate, pH-complexonometric titration, ionic equilibrium.

1. Introduction

Isopolyniobotungstate anions (IPNTA) $H_xNb_2W_4O_{19}^{(4-x)-}$, $x = 0 – 2$ have proven potential in prevention of cellular adsorption of viruses and viral bodies. Thus, IPNTA can serve as a viral fusion inhibiting component of complex anti-virus, anti-tumor and HIV-treatment pharmaceuticals.[1] Besides, they can form stable coordination compounds with transition metals, thus allowing to use them and their derivatives as the ligands in organometallic complexes.[2,3]

But the question of namely $H_xNb_2W_4O_{19}^{(4-x)-}$, $x = 0 – 2$ ions formation in solution is still actual. The most common procedure, that was developed by Dabbabi and Boyer,[4] and still used nowadays, assumes the preparation of the mixed Na–K–NBu$_4$ salts with $Nb_2W_{6-n}O_{19}^{(2+n)-}$, $n = 1 – 4$

anions by mixing of sodium tungstate and an excess of potassium perniobate, followed by acidification of the obtained solution and, finally, the desired product was precipitated by tetrabutylammonium bromide. The authors indicate, that this approach leads to the product, being contaminated by the salts with anions possessing other ratio between *Nb* and *W*. This is because the *pH* regions of different IPNTA domination are overlapped at that conditions.

To avoid the formation of such an impurities, firstly, the synthesis must be carried out at the fixed acidity (*Z*) values. Secondly, only ortho- and hexatungstates of alkali metals should be used, avoiding any use of peroxides or other auxiliary compounds. And thirdly, only precisely stoichiometric ratio between *Nb* and *W* will ensure the formation of the target product.

Two latter issues are easy to solve, but for the first issue one needs to know the acidity regions of predominant formation of IPNTA with the desired composition. To define the correct acidity regions, the state of the ions in aqueous solution must be studied. To the best of our knowledge, these studies were not carried out till now, what can be explained by enormous number of consequtively-parallel reactions, occurring in such systems, and by imperfectness of mathematical methods at that time, that did not allow to estimate qualitative and quantitative composition of the anions in solution. Modern methods of mathematical modeling (MMM) make it possible to solve such problems accurately by interpretation of the experimental data obtained from investigation of interactions in aqueous solutions of IPNTA.

In the present work we studied the formation of the complexes in the system $Nb_6O_{19}^{8-} - WO_4^{2-} - H^+ - H_2O$ (C_{Nb} : C_W = 2 : 4) by *pH*-potentiometric titration and the regions of existence for the forming IPNTA were determined. These allowed us to prepare the compounds with Nb : W = 2 : 4, that does not contain the impurities of the salts with other IPNTA. This was achieved by using the solutions of sodium orthotungstate, potassium hexaniobate and hydrochloric acid. Moreover, no hydrogen peroxide has been used.

2. Experimental

2. 1. Solutions Preparation

The initial solutions were prepared from solids or from concentrated solutions by diluting with distilled water, purified from CO_2. Potassium hexaniobate solution was prepared by dissolving of freshly prepared salt $4K_2O \cdot 3Nb_2O_5 \cdot 12H_2O$. It was prepared by annealing of Nb_2O_5 with 5-fold excess of KOH, followed by thorough washing with the distilled water and double recrystallization from acetone. Sodium tungstate and sodium chloride solutions were prepared by dissolving of solids in water, and the solution of hydrochloric acid was prepared by diluting of the concentrated (10M) solution. The precise concentrations of initial solutions were determined according to chemical analysis data: the contents of tungsten and niobium were determined gravimetrically (gravimetric forms WO_3 and Nb_2O_5, $\delta \leq \pm 0.5\%$), hydrochloric acid was standardized by titration of $Na_2B_4O_7 \cdot 10H_2O$ with methyl red indicator, $\delta \leq \pm 0.8\%$.

2. 2. Complexonometric Titration

The studies of the complexes formation in the system $Nb_6O_{19}^{8-} - WO_4^{2-} - H^+ - H_2O$ were carried out by *pH*-complexonometric titration at 25 ± 0.1°C, using I-500 (Aquilon, Russia) ionometer. Indicator electrode was hydrogen-ion selective glass electrode ESL 63–07 Sr (Belarus) with isopotential point pH_s = 7.00 and $Å_s$ = −25 ± 10

mV, auxiliary electrode EVL-1M3 was silver chloride electrode (Ag/AgCl, sol. KCl, saturated) with the potential of 202 ± 2 mV, according to standart hydrogen electrode. Calibration and preciseness of the readings were controlled by the series of standard buffer solutions, prepared according to Bates.[5] In the systems under investigation the overall concentrations of Nb + W (C^0_{Nb+W}) were 10, 5, 2.5 and 1 mmol/L (mM) and C_{Nb} : C_W = 2 : 4.

The acidity of the systems during titration $Z = C^0_{H^+}/C^0_{Nb+W}$ ($C^0_{H^+}$ is the overall concentration of acid and C^0_{Nb+W} is the overall concentration of niobium and tungsten in solution) was controlled by the amount of the acid being added with step ΔZ = 0.02 within the interval Z = 0 ÷ 2. The ionic strength was created by the background electrolyte (NaCl) and was varied within I = 0.01 ÷ 1.00.

2. 3. Experimental data treatment

For interpretation of experimental data, the mathematical modeling, using CLINP 2.1[6] software, was utilized. Each model was evaluated for consistency with the experimental data. The models were checked for adequateness and excessness, and the main criterium of calculation results coherence with the experimental data was the value of *F*, that is the sum of squares of deviations between calculated and experimental values of *pH* along the entire titration curve:

$$F = \sum_{i=1}^{k} (\Delta pH_i)^2 = \sum_{i=1}^{k} (pH_i^{calc} - pH_i^{exp})^2$$

where *k* is the number of points in the titration curve. It is worth to notice, that the titration considered to be successful, if any point was within $|\Delta pH_i| \leq 0.12$.

The result of mathematical modeling was the determination of concentrational formation constants (lgK_C) for the anions in solution. Based on the obtained values, thermodynamic formation constants $lgK°$ for individual IPNTA were calculated by Pitzer method.[7–9] It is based on the Debai-Huckel equation (*Equation 1*), that has been expanded by the insertion of γ_i-coefficients.[8] They allow to consider the influence of different kinds of ions on each other (*Equations 2 and 3*):

$$lg K_C = lg K^0 - \sum_{i=1}^{s} \nu_i lg \gamma_i \qquad (1)$$

$$lg \gamma_i \approx \frac{1}{\ln 10}\left(z_i^2 \cdot f^{\gamma} + 2\sum_{l=1}^{N} m_i \lambda_{il} + 2\sum_{j=1}^{NK}\sum_{k=1}^{NA} m_j m_k \lambda'_{jk} \right) \qquad (2)$$

$$f^{\gamma} = -A^{\varphi}\left(\frac{\sqrt{I}}{1+b\sqrt{I}} + \frac{2}{b}\ln\left[1+b\sqrt{I}\right] \right) \qquad (3)$$

For equations (1) – (3): A^{φ} is Debai-Huckel coefficient for osmotic function (A^{φ} = 0.3921 at *T* = 298 K); *b* is

the parameter for Pitzer model; I is the ionic strength of solution; m_j and m_k are the molal concentrations of the background electrolyte (j denotes cation and k denotes anion); NK and NA are the numbers of cation and anion correspondingly; N is the overall number of background ions; z_l is the charge of l-ions; λ_{il} and λ'_{jk} are the calculated values that include the parameters describing the interaction between ions.[7]

Calculation of the formation constants allowed to build the distribution diagrams and to determine the regions of predominant formation of the desired IPNTA. These gave a background to create the procedure for thallium salt synthesis. Furthermore, in these regions at the fixed Z and $C_{Nb} : C_W$ values, the solid phase was precipitated. This phase either was the individual salt with $H_xNb_2W_4O_{19}^{(4-x)-}$ anion, or was the mixture of salts with two different x values.

2. 4. Thallium Salts Synthesis

33.7 mL of potassium hexaniobate solution (C_{Nb} = 99 mM) was diluted with 955.5 mL of H_2O and 11.0 mL of sodium orthotungstate solution (C_W = 607 mM) were added dropwise at room temperature with stirring to obtain the solution with $C_{Nb} : C_W$ = 2 : 4. Thus, the set of six solutions was prepared.

Three of the obtained solutions were acidified by the aqueous hydrochloric acid (C_{HCl} = 464 mM) till the desired Z was reached (Step 1 in *Table 1*) and, 1.5-fold excess of thallium (I) nitrate solution (C_{Tl} = 330 mM) was added dropwise at vigorous stirring (Step 2 in *Table 1*).

tion, washed with cold water and dried until constant mass in open air.

The composition of the solid phases were determined by various means of chemical analysis, following the procedure described below. A 500 mg sample of each thallium salt obtained was treated with the 3:1 *v/v* mixture of HNO_3 (70%) and HCl (36%) during 2 hours at stirring. The solid residue, that is $Nb_2O_5 \cdot nH_2O$ and $WO_3 \cdot H_2O$, was filtered, and all the thallium remained in solution. After the solid was annealed for 2 h at 800 °C, the obtained mixture of Nb_2O_5 and WO_3, was heated with $(NH_4)_2SO_4$ in concentrated sulfuric acid (98% *w/w*). The obtained melt was then dissolved in 2% aqueous solution of *EDTA* and *pH* was brought to 8.0 by aqueous ammonia. The suspension was brought to boil and filtered hot after 30 min. Finally, the isolated $Nb_2O_5 \cdot nH_2O$ was annealed at 900 °C until constant mass. Gravimetric form – Nb_2O_5, $\delta \leq \pm$ 0.5%. The weight of WO_3 was found as a difference between the mass of the solid after the first annealing and the mass of Nb_2O_5.

The contents of thallium in the filtrate were determined by the reverse complexonometric titration of the excess of Trilon B by the standard (25 mM) solution of $ZnCl_2$ using xylynol orange as an indicator, $\delta \leq \pm 0.8\%$. The contents of crystallization water were determined by annealing of the sample at 500 °C until constant mass ($\delta \leq \pm$ 0.5%).

The anion identification was based on Fourier-transform infra-red (FTIR) and energy-dispersion X-Ray (EDX) spectroscopic data. FTIR spectra of thallium salts were obtained in KBr pellets, using Thermo Nicolet IR

Table 1. Amounts of solutions, used in thallium salts synthesis.

	Reagent Z	*1.13*	*1.31*	*1.60*
Step 1	V_{HCl}, mL	24.3	28.2	34.5
Step 2	V_{Tl}, mL	30.3	22.7	15.2
Step 3	V_{buffer}, mL	5.0 (buffer **1**)	8.0 (buffer **2**)	5.0 (buffer **3**)

Another three solutions were acidified in the same way, but then the acetate buffer solutions (*Table 2*) were added (Step 3 in *Table 1*), followed by thallium nitrate addition (Step 2 in *Table 1*). The buffer solutions were prepared using 2M solution of sodium acetate and 2M solution of acetic acid.

The obtained heterogenous mixtures were stirred for 5 h, then the white precipitation was separated by filtra-

300 spectrometer within the range of 400–4000 cm^{-1}. EDX analysis was conducted by means of JSM 6490 LV scanning electron microscope (SEM) instrument, using aluminium stand and the carbon film as a support.

3. Results and Discussion

For the system $Nb_6O_{19}^{8-}-WO_4^{2-}-H^+-H_2O$ with C_{Nb+W}^0 = 10, 5, 2.5, 1 mM and $C_{Nb} : C_W$ = 2 : 4, *pH*-potentiometric titration was carried out at the ionic strengths I lying within the range of 0.01 ÷ 1.00 and created by NaCl. It turned out that the general titration curves behaviour does not depend on the ionic strength at given C_{Nb+W}^0. Therefore, it is enough to have just one typical curve for each concentration C_{Nb+W}^0 (*Figure 1*). Moreover, in case of $C_{Nb+W}^0 \geq 5$ mM,

Table 2. Acetate buffer solutions preparation.

Buffer	V (CH$_3$COONa), mL	V (CH$_3$COOH), mL	pH
1	5.0	1.0	5.46
2	1.0	7.4	3.59
3	0.1	20.8	2.36

the ionic strength needed is one order of magnitude higher than C^0_{Nb+W}.

All the titration curves contain two characteristic *pH* gaps, that correspond to the protonation with subsequent polycondensation of the initial tungsten and niobium containing anions. It is worth to notice, that, with the decrease of C^0_{Nb+W}, *pH* gaps become less vivid, especially the one, corresponding to the higher *Z* in solution. The analysis of Z_{theor} of different polyanionic forms of tungsten and niobium formation allows to assume, that the first gap ($Z < 0.3$) may correspond to the protonation of the initial $Nb_6O_{19}^{8-}$:

$$mH^+ + Nb_6O_{19}^{8-} \leftrightarrow H_mNb_6O_{19}^{(8-m)-}$$
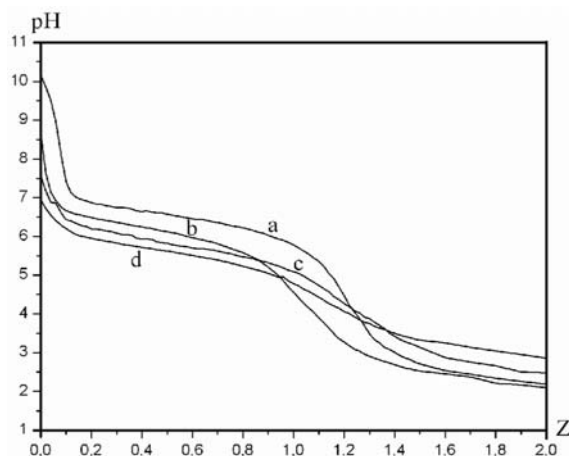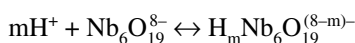
Figure 1. pH-potentiometric titration curves: **a)** C^0_{Nb+W} = 10 mM, I = 500; **b)** C^0_{Nb+W} = 5 mM, I = 140; **c)** C^0_{Nb+W} = 2.5 mM, I = 50; **d)** C^0_{Nb+W} = 1 mM, I = 50.

The second gap ($Z > 0.6$) may correspond either to the polycondensation of the initial WO_4^{2-} into $W_6O_{20}(OH)_2^{6-}$, $W_{12}O_{40}(OH)_2^{10-}$ and $HW_7O_{24}^{5-}$, or to the formation of the mixed IPNTA with the niobium contents being higher than that, determined by the initial feed $C_{Nb} : C_W = 2 : 4$:

$$\frac{n}{6}Nb_6O_{19}^{8-} + (6-n)WO_4^{2-} + \frac{30-5n+3x}{3}H^+ \leftrightarrow$$

$$\leftrightarrow H_xNb_nW_{6-n}O_{19}^{(2+n-x)-} + \frac{30-5n}{6}H_2O, n \leq 3$$
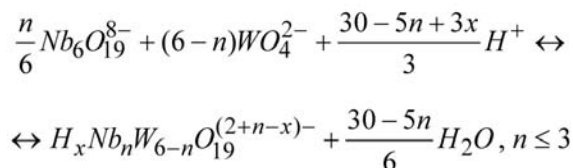
In this case one might expect that the processes of protonation take place consequently and can be easily assigned. Whatsoever, the processes of tungstate anions polycondensations are more complicated and, according to the recent data,[10] proceed through consecutive–parallel schemes. It is also possible, that consecutive–parallel hypothesis can be applied to IPNTA, especially because in parallel reaction there forms a complex with higher nio-

bium contents than expected, as it was observed in similar tungsten–niobium systems with $C_{Nb} : C_W = 1 : 5.$[11]

Such assumptions inambigously indicate the problem of experimental data interpretation and reveal the impossibility of truthful explanation of gaps in the $pH = f(Z)$ curves, if based only on the theoretical values of *Z* for both individual and mixed isopoly anions. Indeed, it is impossible to build the schemes of ions interchange and to calculate the formation constants of IPNTA. Thus, to treat the experimental data, the method of mathematical modeling was used. This allows to find the models that adequately describe the complexation processes in the studied systems.

The modeling of these systems was started from assuming the presence of only mixed isopoly anions $H_xNb_2W_4O_{19}^{(4-x)-}$, $x = 0 - 2$, with the ratio between niobium and tungsten being determined by the initial solutions. As a result, the proposed model (*Model 1*) contained only three anions ($Nb_2W_4O_{19}^{4-}$, $HNb_2W_4O_{19}^{3-}$ and $H_2Nb_2W_4O_{19}^{2-}$) and could satisfactorily describe (with $\Delta pH \leq 0.12$) the experimental data for $Z > 1.6$ (*Figure 2a*), and thus was discarded.

Then, individual IPNTA $W_6O_{20}(OH)_2^{6-}$ and $HW_7O_{24}^{5-}$ were added to *Model 1*, and the *Model 2* was created. This allowed to expand the adequacy region for calculated *pH* values from $Z > 1.6$ to $Z > 1.2$ (*Figure 2b*). So, *Model 2* describes well the processes at high *Z*, but at low $Z < 1.2$ the error exceeds the accepted value ($\Delta pH \leq 0.12$). If other tungsten anions, such as $W_7O_{24}^{6-}$, $W_{12}O_{40}(OH)_2^{10-}$, $W_{12}O_{38}(OH)_2^{6-}$, $W_{10}O_{32}^{4-}$ were used in *Model 2*, it did not change the region of experimental and calculated pH values coincidence, but negatively affected other model parameters, clearly indicating the excessiveness of the proposed model and the subsequent excluding latter mentioned particles.

When the mixed isopoly anion $Nb_3W_3O_{19}^{5-}$ was added to the *Model 2*, the *Model 3* was obtained. This anion seemed to be the only one to help eliminate uncertainty in the region of the middle *Z* values. The results (*Figure 2c*) showed that satisfactory coincidence of experimental and calculated *pH* values was observed in relatively wide region $Z > 0.6$. But, at lower *Z* values this model was still not correspondent to the real process.

Finally, when protonated anions of niobium, $HNb_6O_{19}^{7-}$ and $H_2Nb_6O_{19}^{6-}$, were added to the *Model 3* to obtain *Model 4*, it correctly described the processes of complex formation in the entire studied *Z* interval, within the error of $\Delta pH \leq 0.12$ (*Figure 2d*).

Aside of the models described, we tried to apply the series of more complicated anions, including other IPNTA, but all of them proved to be invaluable and/or excessive. Indeed, all subsequent calculations at all the concentrations and ionic strengths used, the *Model 4* was chosen as a reference.

From one side, the chemical nature of this model includes well-studied protonation processes of hexaniobo-
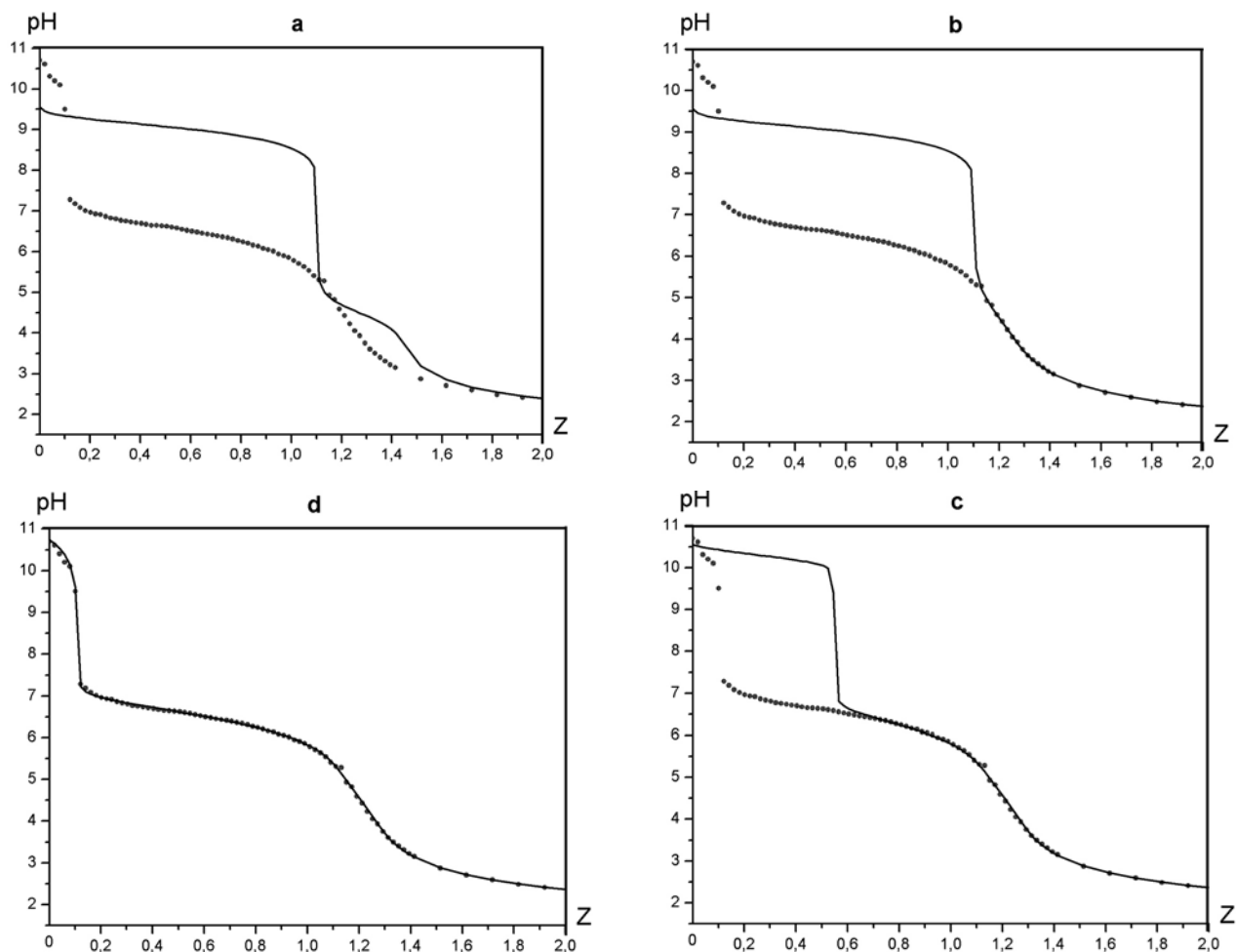
Figure 2. Step-by-step mathematic modeling of the system $Nb_6O_{19}^{8-}$–WO_4^{2-}–H^+–H_2O with $C_{Nb+W}^0 = 10$ mM, experimental (dots) and calculated (solid line) curves: **a**) – Model 1: ions $Nb_2W_4O_{19}^{4-}$, $HNb_2W_4O_{19}^{3-}$ and $H_2Nb_2W_4O_{19}^{2-}$; **b**) – Model 2: ions $Nb_2W_4O_{19}^{4-}$, $HNb_2W_4O_{19}^{3-}$, $H_2Nb_2W_4O_{19}^{2-}$, $HW_7O_{24}^{5-}$ and $W_6O_{20}(OH)_2^{6-}$; **c**) – Model 3: ions $Nb_2W_4O_{19}^{4-}$, $HNb_2W_4O_{19}^{3-}$, $H_2Nb_2W_4O_{19}^{2-}$, $Nb_3W_3O_{19}^{5-}$, $HW_7O_{24}^{5-}$ and $W_6O_{20}(OH)_2^{6-}$; **d**) – Model 4: ions $Nb_2W_4O_{19}^{4-}$, $HNb_2W_4O_{19}^{3-}$, $H_2Nb_2W_4O_{19}^{2-}$, $Nb_3W_3O_{19}^{5-}$, $HW_7O_{24}^{5-}$, $W_6O_{20}(OH)_2^{6-}$, $HNb_6O_{19}^{7-}$ and $H_2Nb_6O_{19}^{6-}$.

tungstate–ions and polycondensation of orthotungstate–ions, with the known formation constants:[12,13]

$$Nb_6O_{19}^{8-} + H^+ \leftrightarrow HNb_6O_{19}^{7-}$$
$$Z = 0.056$$
$$(\lg K_C = 11.90)$$

$$Nb_6O_{19}^{8-} + 2H^+ \leftrightarrow H_2Nb_6O_{19}^{6-}$$
$$Z = 0.11$$
$$(\lg K_C = 22.90)$$

$$6WO_4^{2-} + 6H^+ \leftrightarrow W_6O_{20}(OH)_2^{6-} + 2H_2O$$
$$Z = 0.67$$
$$(\lg K_C = 50.41)$$

$$7WO_4^{2-} + 9H^+ \leftrightarrow HW_7O_{24}^{5-} + 4H_2O$$
$$Z = 0.86.$$
$$(\lg K_C = 70.70)$$
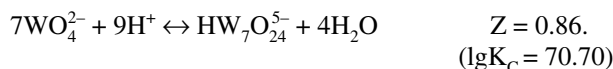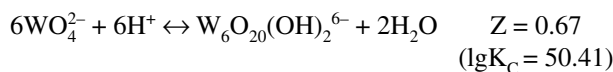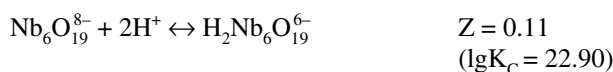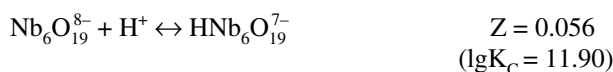
From the other side, the model contains the equilibrium processes of IPNTA formation, whose constants were unknown till now:

$$Nb_6O_{19}^{8-} + 12WO_4^{2-} + 20H^+ \leftrightarrow 3Nb_2W_4O_{19}^{4-} + 10H_2O$$
$$Z = 1.11$$

$$Nb_6O_{19}^{8-} + 12WO_4^{2-} + 23H^+ \leftrightarrow 3HNb_2W_4O_{19}^{3-} + 10H_2O$$
$$Z = 1.28$$

$$Nb_6O_{19}^{8-} + 12WO_4^{2-} + 26H^+ \leftrightarrow 3H_2Nb_2W_4O_{19}^{2-} + 10H_2O$$
$$Z = 1.44$$

$$Nb_6O_{19}^{8-} + 6WO_4^{2-} + 10H^+ \leftrightarrow 2Nb_3W_3O_{19}^{5-} + 5H_2O$$
$$Z = 0.56$$
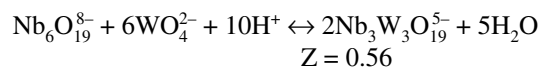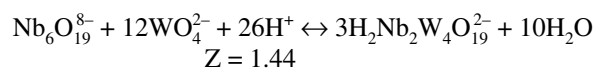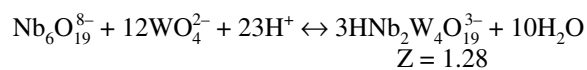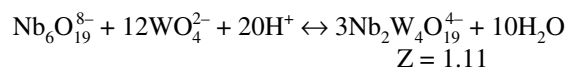
The formation constants for isopolytungstates and isopolyniobates were introduced into the model as fixed values, and the average values of formation constants for the mixed IPNTA were calculated during modeling for all the concentrations at the correspondent ionic strengths (*Table 2*).

The complete set of concentrational formation constants allowed us to calculate the concentrations of anions and to build the distribution diagrams for the ionic forms (mol % α as a function of acidity Z) at C_{Nb+W}^0 = 10, 5, 2.5, 1 mM and varying ionic strengths. Since the diagrams for different ionic strengths do not change for particular concentration, we illustrated the general behaviour at one ionic strength for simplicity (*Figure 3*).

me the existence of the variety of the protonated forms of both initial $Nb_6O_{19}^{8-}$ and final $Nb_2W_4O_{19}^{4-}$ ($H_xNb_2W_4O_{19}^{(4-x)-}$, $x = 0 – 2$) anions, as it follows from mathematical model. Lowering the concentration decreases the degree of protonation of the final anion ($H_xNb_2W_4O_{19}^{(4-x)-}$, $x = 0 – 1$) and the protonated forms appear only at higher values of ionic strength. In the diluted systems, where C_{Nb+W}^0 = 1 mM, isopoly forms of niobium and tungsten interact with each

Table 2. Average values of concentrational constants logarithms for the mixed IPNTA at different ionic strengths. Values in brackets denote RMS deviation.

Ionic Strength,	Concentrational constants, lgK_C (S)			
I, mol/L	$Nb_2W_4O_{19}^{4-}$	$HNb_2W_4O_{19}^{3-}$	$H_2Nb_2W_4O_{19}^{2-}$	$Nb_3W_3O_{19}^{5-}$
0,01	51,96 (0,14)	–	–	–
0,02	51,98 (0,13)	–	–	–
0,03	51,85 (0,12)	–	–	41,16 (0,08)
0,04	51,83 (0,13)	55,93 (0,13)	–	40,63 (0,14)
0,05	51,44 (0,10)	–	–	–
0,06	51,59 (0,11)	55,60 (0,13)	–	40,08 (0,18)
0,07	51,16 (0,13)	55,94 (0,10)	–	40,68 (0,12)
0,08	51,54 (0,11)	–	–	40,92 (0,12)
0,09	–	–	–	40,17 (0,18)
0,10	52,44 (0,12)	56,05 (0,18)	–	40,51 (0,16)
0,12	–	–	–	41,99 (0,17)
0,14	52,60 (0,15)	55,98 (0,16)	–	43,35 (0,16)
0,16	53,05 (0,14)	56,62 (0,14)	–	43,76 (0,14)
0,18	52,57 (0,17)	55,85 (0,17)	–	43,72 (0,15)
0,20	54,52 (0,11)	59,16 (0,11)	–	43,80 (0,15)
0,30	54,81 (0,10)	59,61 (0,10)	–	43,87 (0,14)
0,40	54,60 (0,10)	–	61,63 (0,16)	43,93 (0,12)
0,50	54,69 (0,12)	–	62,04 (0,20)	43,94 (0,15)
0,60	54,76 (0,12)	–	62,59 (0,16)	44,06 (0,14)
0,80	54,33 (0,12)	–	61,39 (0,23)	43,91 (0,14)
1,00	54,29 (0,12)	–	61,50 (0,20)	43,79 (0,15)

According to the distribution diagrams, the region of the first gap correspond to the protonation process of the initial $Nb_6O_{19}^{8-}$, that totally agrees with Z_{theor}. In parallel to this process, the polycondensation of the initial WO_4^{2-} takes place, that leads to $W_6O_{20}(OH)_2^{6-}$ formation. As soon as the tungstate-anions, that possess the same as $Nb_6O_{19}^{8-}$ oxygen coordination of the metal, appear in solution, the formation of IPNTA, i.e. $Nb_3W_3O_{19}^{5-}$, begins. The deficit of tungsten in this form, if compared with the most expected $Nb_2W_4O_{19}^{4-}$ could be possibly explained by insufficient tungsten isopoly anions formation at lower Z. Notably, when reaching $Z \geq 0.8$ (Z_{theor} = 0.86), in parallel with the above mentioned processes, $HW_7O_{24}^{5-}$ appears in the solution. Along with $W_6O_{20}(OH)_2^{6-}$ and $Nb_3W_3O_{19}^{5-}$, it takes part in the formation of the expected $Nb_2W_4O_{19}^{4-}$. The latter, as the acidity of the system grows, undergoes step-by-step protonation to give $H_xNb_2W_4O_{19}^{(4-x)-}$, $x = 0 – 2$.

Even though the processes of complexes formation in the system $Nb_6O_{19}^{8-}–WO_4^{2-}– H^+– H_2O$ at different C_{Nb+W}^0 are general, there exist certain peculiarities, characteristic for each concentration. Thus, at C_{Nb+W}^0 = 10 mM we presu-

other, giving $Nb_2W_4O_{19}^{4-}$ without intermediate formation of $Nb_3W_3O_{19}^{5-}$.

The average values of concentrational constants (*Table 2*), calculated at different concentrations and the same ionic strength, allowed to calculate thermodynamic formation constants of mixed IPNTA (*Table 3*). The calculations were carried out by Pitzer method using extrapolation of lgK_C dependence to the zero value of ionic strength.

Following the distribution diagrams for the anions in the studied systems at C_{Nb+W}^0 = 10 mM, we isolated the solid phases in the regions of predominant formation of $H_xNb_2W_4O_{19}^{(4-x)-}$, $x = 0 – 2$ ions (*Table 4*).

Table 3. Thermodynamic constants of the mixed IPNTA formation.

Anion	Thermodynamic constants, $lgK°$
$Nb_2W_4O_{19}^{4-}$	54.39 ± 0.24
$HNb_2W_4O_{19}^{3-}$	60.83 ± 0.68
$H_2Nb_2W_4O_{19}^{2-}$	67.04 ± 0.67
$Nb_3W_3O_{19}^{5-}$	41.68 ± 0.42
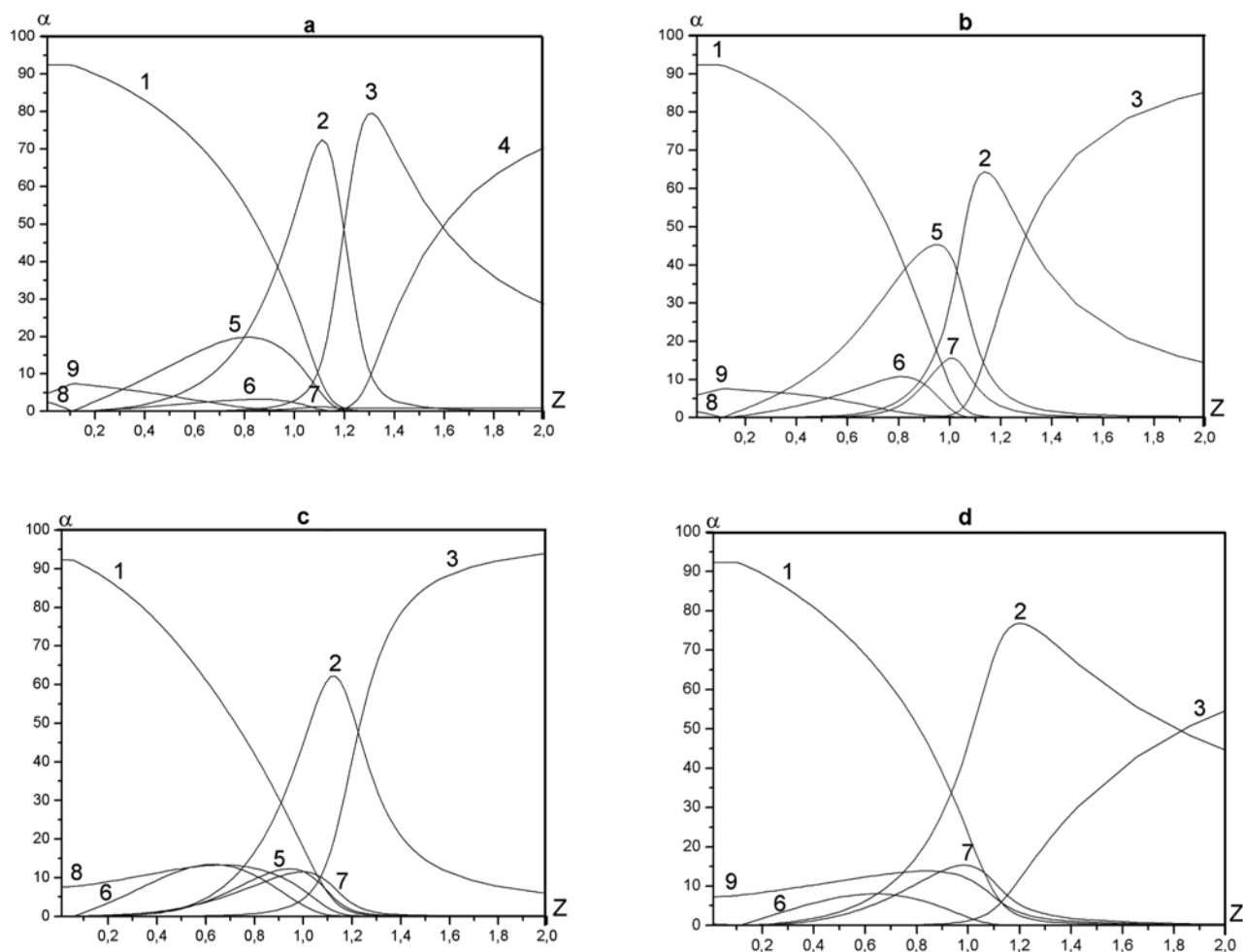
Figure 3. Diagrams of ions distribution in the system $Nb_6O_{19}^{8-}$–WO_4^{2-}–H^+–H_2O at different concentrations: **a)** $C_{Nb+W}^0 = 10$, I = 500; **b)** $C_{Nb+W}^0 = 5$, I = 140; **c)** $C_{Nb+W}^0 = 2.5$, I = 50; **d)** $C_{Nb+W}^0 = 1$, I = 50. In these charts: **1** – WO_4^{2-}, **2** – $Nb_2W_4O_{19}^{4-}$, **3** – $HNb_2W_4O_{19}^{3-}$, **4** – $H_2Nb_2W_4O_{19}^{2-}$, **5** – $Nb_3W_3O_{19}^{5-}$, **6** – $W_6O_{20}(OH)_2^{6-}$, **7** – $HW_7O_{24}^{5-}$, **8** – $HNb_6O_{19}^{7-}$, **9** – $H_2Nb_6O_{19}^{6-}$.

In case of $H_2Nb_2W_4O_{19}^{2-}$ and $HNb_2W_4O_{19}^{3-}$ there is a substantial overlapping of the regions of the anions existence, and this dictated the use of higher acidity than calculated for $H_2Nb_2W_4O_{19}^{2-}$.

Preliminary investigations revealed that *pH* of the mother liquor decreases dramatically during cation addition and formation of heterogenous system (*Table 4*). This leads to the case, when, instead of expected $H_xNb_2W_4O_{19}^{(4-x)-}$, there forms the mixture of its salt with

the compound, containing $H_{x+1}Nb_2W_4O_{19}^{(3-x)-}$. Fortunately, this was not the case at $Z = 1.60$, when the only salt with the desired anion $H_2Nb_2W_4O_{19}^{2-}$ was formed.

To avoid such a decrease in *pH*, the acetate buffers were used. Their *pH* was adjusted in accordance to the *Figure 1* for the needed Z. In these buffers the series of thallium salts were obtained and analyzed for the contents of the main constituents: Tl_2O, Nb_2O_5, $WO_3 \cdot H_2O$ (*Tables 5 and 6*).

The chemical analysis of the synthesized thallium salts allowed to suggest the following molecular formulas: $Tl_3HNb_2W_4O_{19} \cdot 10H_2O$ and $Tl_2H_2Nb_2W_4O_{19} \cdot 10H_2O$. The presence of the anions $H_xNb_2W_4O_{19}^{(4-x)-}$ was evidenced by FTIR spectroscopy. The following bands at $951(\nu_{W=O})$, $895(\nu_{Nb=O})$, 800, 694, 568 and 400 ($\nu_{M-O-M} \cdot \delta_{M-O-M}$) cm^{-1} clearly indicate on the substructure M_6O_{19}, as it was described by Rocchiccioli-Deltcheff *et al.*[14] and Anderson *et al.*[15]

Table 4. Parameters of IPNTA isolation.

Anion	Z_{exp}	Z_{theor}	mol % in solution
$Nb_2W_4O_{19}^{4-}$	1.13	1.11	71
$HNb_2W_4O_{19}^{3-}$	1.31	1.28	79
$H_2Nb_2W_4O_{19}^{2-}$	1.60	1.44	42

Table 5. Chemical analysis data for the salts, being precipitated from solutions without using a buffer solution.

Z = 1.13	Tl_2O	Nb_2O_5	WO_3	H_2O
Found, %	33.95	12.61	44.00	9.14
Calculated for	33.89	12.66	44.17	9.00
$0.35Tl_4Nb_2W_4O_{19} + 0.65Tl_3HNb_2W_4O_{19}$, %				

Z = 1.31	Tl_2O	Nb_2O_5	WO_3	H_2O
Found, %	27.58	13.77	47.56	9.79
Calculated for	27.50	13.77	48.03	10.00
$0.5Tl_3HNb_2W_4O_{19} + 0.5Tl_2H_2Nb_2W_4O_{19}$, %				

Z = 1.60	Tl_2O	Nb_2O_5	WO_3	H_2O
Found, %	21.58	14.52	51.64	9.68
Calculated for	23.63	14.78	51.57	10.02
$Tl_2H_2Nb_2W_4O_{19}9H_2O$, %				

Table 6. Chemical analysis data for the salts, being precipitated from solutions, using acetate buffer solution.

	Tl_2O	Nb_2O_5	WO_3	H_2O
Found, %	35.25	11.97	42.81	8.85
Calculated for				
$0.7Tl_4Nb_2W_4O_{19}+0.3Tl_3HNb_2W_4O_{19}$, %	37.91	11.86	41.38	8.85
	Tl_2O	Nb_2O_5	WO_3	H_2O
Found, %	31.94	13.42	46.53	9.51
Calculated for				
$Tl_3HNb_2W_4O_{19}10H_2O$, %	31.55	13.16	45.92	9.37
	Tl_2O	Nb_2O_5	WO_3	H_2O
Found, %	22.13	14.34	50.42	11.01
Calculated for				
$Tl_2H_2Nb_2W_4O_{19}10H_2O$, %	23.39	14.63	51.06	10.91

SEM images of thallium salt powders (*Figure 4*) show that there are no zones with different surface morphology and EDX spectral analysis in single spots and different zones with area from 24 × 14.4 to 66.8 × 49.9 μm exhibit no substantial deviation from the ratio Nb : W = 2 : 4. These clearly indicate the formation of monophase samples of $Tl_{4-x}H_xNb_2W_4O_{19}$, and not the mixture of $Tl_{3-x}H_xNbW_5O_{19}$ and $Tl_{5-x}H_xNb_3W_3O_{19}$. The analogous SEM and EDX results were also obtained for all the thallium salts, described in *Tables 5* and *6*. The compound $Tl_2H_2Nb_2W_4O_{19} \cdot 10H_2O$ was chosen to serve as an example.
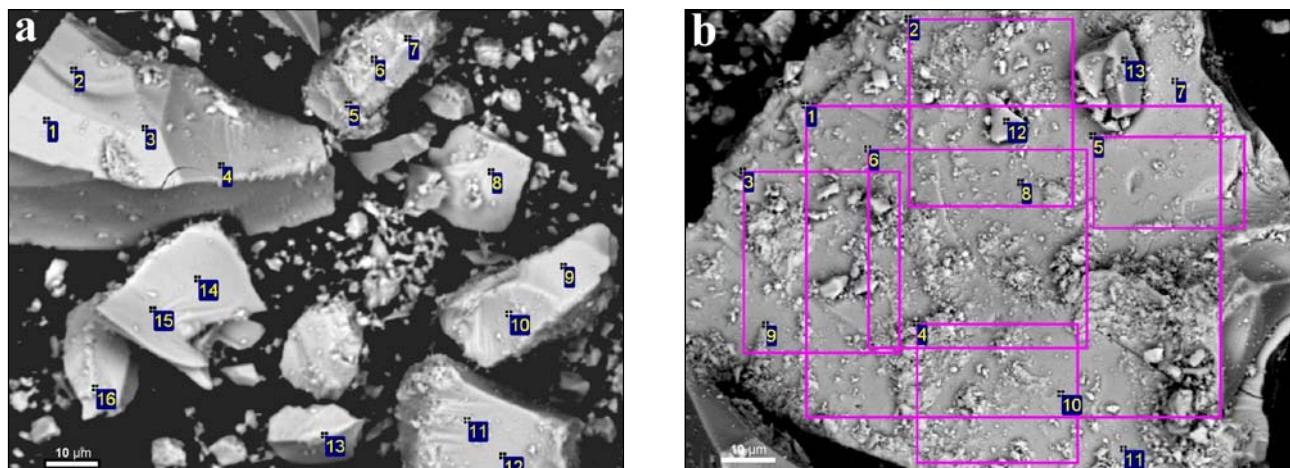
Figure 4. SEM images of the morphology of $Tl_2H_2Nb_2W_4O_{19} \cdot 10H_2O$ powder. Compositional spectral analysis was made in single spots and zones indicated (See *Table 7*).
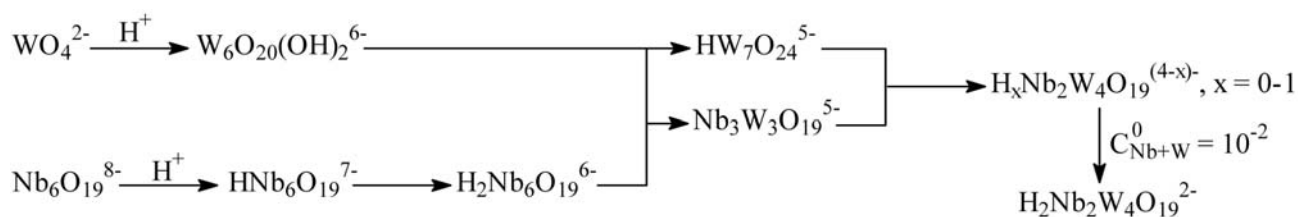
Scheme 1. Possible anions transformations in the system $Nb_6O_{19}^{8-}$–WO_4^{2-}–H^+–H_2O.

Table 7. Molar ratio Nb:W in different spots and zones of $Tl_2H_2Nb_2W_4O_{19} \cdot 10H_2O$ powder.

Image *a*	N_{Nb}*	N_W	Image *b*	N_{Nb}*	N_W
spot 1	2	3.89	zone 1	2	4.05
spot 2	2	4.07	zone 2	2	3.95
spot 3	2	3.93	zone 3	2	4.02
spot 4	2	3.92	zone 4	2	3.96
spot 5	2	4.09	zone 5	2	4.03
spot 6	2	4.15	zone 6	2	3.99
spot 7	2	3.89	spot 7	2	3.93
spot 8	2	4.08	spot 8	2	3.98
spot 9	2	3.89	spot 9	2	3.84
spot 10	2	3.85	spot 10	2	3.89
spot 11	2	4.12	spot 11	2	4.00
spot 12	2	3.91	spot 12	2	3.96
spot 13	2	4.07	spot 13	2	3.89
spot 14	2	4.08			
spot 15	2	4.05			
spot 16	2	3.98			

* – the ratio was recalculated for 2 atoms of *Nb* for simplicity

4. Conclusions

To finalize, mathematical modeling allowed us to adequately interpret the experimental results and to suggest the following sequence of parallel-consequent processes in the system $Nb_6O_{19}^{8-}$–WO_4^{2-}–H^+–H_2O with C_{Nb} : $C_W = 2 : 4$ (*Scheme 1*).

5. References

1. J. T. Rhule, C. L. Hill, D. A. Judd *Chem. Rev.* **1998**, *98*, 327–358.
2. C. Besecker, W. G. Klemperer, V. W. Day *J. Am. Chem. Soc.* **1982**, *104*, 6158–6159.
3. V. W. Day, T. A. Eberspacher, W. G. Klemperer, R. P. Planalp, P. W. Schiller, A. Yagasaki, B. Zhong *Inorg. Chem.* **1993**, *32*, 1629–1637.
4. M. Dabbabi, M. Boyer *J. Inorg. Nucl. Chem.* **1976**, *38*, 1011–1014.
5. R. Bates pH Determination. Theory and practice (Book), *Khimija*, *Leningrad* **1968**, 94–124 (*in Russian*).
6. Y. Kholin Quantitative physico-chemical analysis of complex formation in solutions and on the surface of the chemically modified silica: models, mathematical methods and their applications (Book), *Folio*, *Kharkov* **2000** (*in Russian*).
7. K. S. Pitzer, G. Mayorga *J. Phys. Chem.* **1973**, *77*, 2300–2308.
8. A. A. Bugaevski, Y. V. Kholin, D. S. Konjaev, A. V. Krasovitski *Zh. Obshch. Khim.* **1998**, *68*, 753–757 (*in Russian*).
9. G. Meinrath *Anal. Bioanal. Chem.* **2002**, *374*, 796–805.
10. J. J. Hastings, O. W. Howarth *J. Chem. Soc. Dalton Trans.* **1992**, 209–215.
11. G. M. Rozantsev, S. M. Vavilova, K. E. Belousova *Rus. J. of Inorg. Chem.* **2007**, *52*, 1478–1485.
12. G. M. Rozantsev, O. I. Sazonova, Y. V. Kholin *Zh. Neorg. Khim.* **1998**, *43*, 1894–1899 (*in Russian*).
13. B. Spinner *Rev. Chim. Miner.* **1968**, *5*, 839–868.
14. C. Rocchiccioli-Deltcheff, R. Thouvenot, M. Dabbabi *Spectrochim. Acta* **1977**, *A33*, *2*, 143–153.
15. Anderson T. M., Rodriguez M. A., Stewart T. A. et al. *Eur. J. Inorg. Chem.* **2008**, 8286–3294.

Povzetek

Potenciometrično smo raziskovali proces nastanka kompleksa $Nb_6O_{19}^{8-}$–WO_4^{2-}–H^+–H_2O pri razmerju C_{Nb} : $C_W = 2 : 4$ ter različnih Nb + W koncentracijah. Eksperimentalne podatke smo analizirali z matematičnim modelom, ki omogoča konstrukcijo porazdelitvenega diagrama posameznih niobijevih in tungstenovih izopoli anionov ter mešanih izopolinio-botungstatov v območju $Z = C_{H^+}^0/C_{Nb+W}^0 = 0 - 2.0$ (ob prisotnosti NaCl). Z uporabo quasi-Neutonove metode (CLINP 2.1 software) smo določili termodinamske tvorbene konstante. Pokazali smo, da te tvorba isopoliniobotungstatov $(H_xNb_2W_4O_{19}^{(4-x)-}, x = 0 - 2)$ v 6. periodi periodnega sistema poteka preko itermediatnih ionov $Nb_3W_3O_{19}^{5-}$. Izolirali smo soli talija $Tl_3hNb_2W_4O_{19} \cdot 10H_2O$ ter $Tl_2H_2Nb_2W_4O_{19} \cdot 10H_2O$ ter jih analizirali z elementno analizo in FTIR spektroskopijo.